

## HEAT AND MASS TRANSFER DURING NONEQUILIBRIUM DECOMPOSITION OF HYDRATE PELLET

Yong Seok Yoon, Myung Ho Song\*

Department of Mechanical Engineering, Dongguk University  
Pil-Dong, Chung-Ku, Seoul, 100-715 KOREA

Jung Ho Kang

Department of Mechanical Engineering, Seoul National University  
Sinlim-Dong, Kwanak-Ku, Seoul, 151-742 KOREA

Peter Englezos

Department of Chemical & Biological Engineering, University of British Columbia  
2360 East Mall, Vancouver, BC, V6T 1Z3 CANADA

### ABSTRACT

Mathematical model, which depicts on macroscopic scale the physical phenomena occurring during the decomposition of gas hydrate, was set up and applied to the spherical methane hydrate pellet decomposing into ice. Initially, porous hydrate pellet is at uniform temperature and pressure within hydrate stable region. The pressure starts to decrease at  $t=0$  with a fixed rate down to the final pressure and is kept constant afterwards. The bounding surface of pellet is heated by convection. Governing equations are based on the conservation principles, the phase equilibrium relation, equation of gas state and phase change kinetics. The single-domain approach and volume average formulation are employed to take into account transient change of local pressure, volumetric liberation of latent enthalpy, and convective heat and mass transfer accompanied by the decomposed gas flow through hydrate/ice solid matrix. The algorithm called "enthalpy method" is extended to deal with non-equilibrium phase change and utilized to determine local phase volume fractions. Predicted results suggest that the present numerical implementation is capable of predicting essential features of heat and mass transfer during non-equilibrium decomposition of hydrate pellet.

*Keywords:* gas hydrates, pellet decomposition, numerical simulation, intrinsic kinetic

### NOMENCLATURE

$A_s$	Surface area [ $m^2$ ]	$h_{eff}$	Convection coefficient [ $W / m^2 K$ ]
$c_p$	Specific heat [ $kJ / kgK$ ]	$K$	Permeability [ $m^2$ ]
$A_s$	Surface area [ $m^2$ ]	$k_{eff}$	Thermal conductivity [ $W / mK$ ]
$C$	Water mass fraction in hydrate phase	$k_o$	Kinetic rate constant [ $kmol / (sm^2 Pa)$ ]
$E$	Activation energy [ $kJ / kmol$ ]	$k_T$	Kinetic rate constant [ $/(sK)$ ]
$f$	Fugacity of gas [ $kPa$ ]	$\bar{M}$	Molecular weight [ $kg / kmol$ ]
$\Delta H$	Surface area [ $m^2$ ]	$n$	Hydration number
$h$	Enthalpy [ $kJ / kg$ ]	$P$	Pressure [ $kPa$ ]
		$Q$	Local mass flow rate [ $kg / s$ ]

\* Corresponding author: Phone: +82 2 2260 3827 Fax +82 2 2263 9379 E-mail: songm@dug.edu

$R$	Radius of pellet [ $m$ ]
$T$	Temperature [ $K$ ]
$t$	Time [s]
$u$	Internal energy [ $kJ / kg$ ]
$V$	Volume [ $m^3$ ]
$v$	Pore velocity [ $m / s$ ]
$\varepsilon$	Phase volume fraction
$\rho$	Density [ $kg / m^3$ ]
<i>Subscript</i>	
$eq$	Equilibrium
$f$	Final value
$G$	Gas
$H$	Hydrate
$I$	Ice
$i$	Initial value
$q1$	Quadruple point
$s$	Surrounding medium

## INTRODUCTION

The decomposition of hydrate occurs in a variety of geophysics and engineering situations including gas recovery from natural hydrate deposit as an energy resource and removing hydrate plugs formed in oil and natural gas pipelines. This work is especially motivated by the need to design the regasification process of pelletized and stored artificial hydrate as an economic alternative for natural gas transportation and storage. [1]

The different methods that can be used to dissociate a hydrate plug in the pipeline or hydrate core in oceanic and permafrost deposits are: depressurization, thermal stimulation, thermodynamic inhibitor injection, or a combination of those. [2] The research attention previously focused on pipeline plug dissociation [3, 4] is lately drawn by gas production from natural hydrate decomposition [5-7]. The detailed and recent reviews of hydrate dissociation models reported in the literature are available. [2, 7]

The objective of the present work is to develop mathematical model which depicts on macroscopic scale the physical phenomena occurring during the decomposition of hydrate packed in spherical pellet into ice. The algorithm called "enthalpy method" is extended to deal with non-equilibrium phase change and utilized to determine local phase volume fractions. The influence of different pellet size, permeability, convective heating from surrounding medium and intrinsic kinetic rate on

the predicted heat and mass transfer during decomposition of hydrate pellet are reported.

## ANALYSIS

### Physical situations and assumptions

The mathematical model of the present study depicts on a macroscopic scale the physical phenomena occurring during the decomposition of spherical hydrate pellet caused by simultaneous depressurization and convective heating. The schematic of physical situation is shown in Fig. 1. Initially, the porous hydrate pellet is saturated with methane, and is at a uniform temperature ( $T_i$ ) below quadruple point temperature ( $T_{q1}$ ), and under uniform pressure ( $P_i$ ) larger than triple phase equilibrium value for the given initial temperature. At some instance of time ( $t=0$ ), the pressure starts to decrease with a fixed rate until the final pressure ( $P_f$ ) is reached, and is maintained constant afterwards. In the mean time, the outer surface of pellet is heated by convective heat gain from surrounding medium. Decomposition of hydrate continues until all hydrate changes into ice because the temperature of the surrounding medium ( $T_s$ ) is higher than triple phase equilibrium temperature corresponding with  $P_f$ .

A careful identification of physical processes is a prerequisite to establishing mathematical models. Since decomposition of hydrate is relevant to the physical phenomena in terms of macroscopic variables. To set up tractable mathematical models, the following assumptions are made.

- The hydrate decomposition and accompanied transport processes are one-dimensional (in radial direction only).
- The thermo-physical properties of hydrate, ice and gas phases are homogeneous, isotropic and independent of the temperature, pressure or composition, but may differ from phase to phase. The exception is the density of gas which is determined by Redlich/Kong EOS. Therefore, thermal expansion and compressibility of condensed phase (hydrate and ice phases) are neglected.
- The latent energy of each phase is also constant and hydration number ( $n$ ) is fixed at 6.0.
- The water vapor within gas phase is ignored, and the solubility of methane in ice is zero.
- The condensed phases are stationary and rigid.

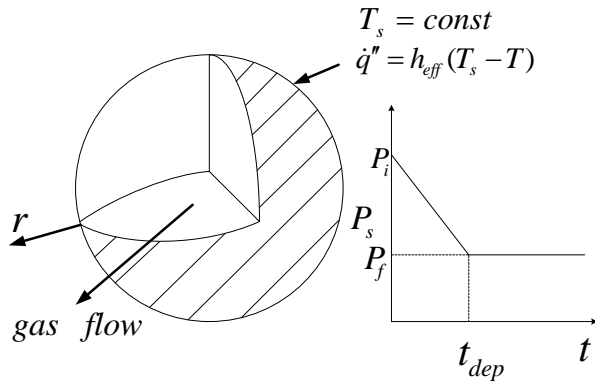


Figure 1 Physical situation

- All phases simultaneously occupying the local volume are under same pressure and in thermal equilibrium.

### Volume averaged model equations

The mathematical model for the dissociation of a porous hydrate is based on the conservation principles, EOS, the phase equilibrium relation and phase change kinetics.

The first choice that has to be made in setting up the macroscopic transport equations for the multi-phase problems is between the multi-domain and single-domain approaches. In the multi-domain approach, different sets of model equations are written for more than one domain, which usually represent regions of different phase combinations, and are coupled through the conditions at the boundaries shared by adjacent domains. The moving boundaries between domains have to be tracked unless they are assumed known or prescribed as part of analytic solutions. The numerical procedure for multi-domain approach generally requires the adaptive grid system which is not necessarily orthogonal.

The single-domain approach is better suited for the hydrate phase change simulation, because it is capable of treating the highly irregular boundaries between regions and of taking into account more realistic features such as volumetric liberation of latent energy, non-uniform distribution of porosity, transient change of local pressure and convective heat and mass transfer accompanied by capillary gas flow through hydrate/ice solid matrix.

The derivation of the macroscopic transport equations for single-domain approach can be made either through the continuum mixture formulation or the volume average formulation. [8] The volume average formulation is selected in the

present study since the derivation is mathematically rigorous, and the basic concepts can be conveniently extended to the treatment of non-equilibrium phase change model. The final forms of the macroscopic transport equations should be the same as those based on the continuum mixture formulation, if the assumptions and the dependent variables are identical.

In the volume average formulation, the macroscopic transport equations are obtained by averaging the microscopic conservation equations over the volume element comprising more than one phase. The averaging volume elements are much smaller than the size of the system and much larger than the characteristic length of the phase interface so that the results of the averaging process may be assumed to be independent of the element size. The detailed volume averaging procedure to derive the general macroscopic transport equations from the microscopic conservation equations together with the average theorems are well documented.[8] The macroscopic transport equations valid under the assumptions made earlier are continuity, momentum equations and energy equation in terms of the phase variables  $\rho_k$ ,  $\varepsilon_k$ , and  $h_k$  written as follows:

$$\text{Continuity: } \frac{\partial}{\partial t} (\varepsilon_G \rho_G + \varepsilon_I \rho_I + \varepsilon_H \rho_H) + \frac{1}{r^2} \frac{\partial}{\partial r} (r^2 \varepsilon_G \rho_G v_G) = 0 \quad (1)$$

$$\text{Momentum: } 0 = -\frac{\partial P}{\partial r} - \frac{\mu_G}{K} (\varepsilon_G \rho_G v_G) \quad (2)$$

Energy:

$$\frac{\partial}{\partial t} (\varepsilon_G \rho_G h_G + \varepsilon_I \rho_I u_I + \varepsilon_H \rho_H u_H) - \frac{\partial}{\partial t} (\varepsilon_G P) + \frac{1}{r^2} \frac{\partial}{\partial r} (r^2 \varepsilon_G \rho_G v_G h_G) = \frac{1}{r^2} \frac{\partial}{\partial r} (r^2 k_{eff} \frac{\partial T}{\partial r}) \quad (3)$$

In the above equations, the subscripts G, I and H represent gas, ice and hydrate phases respectively and  $v_g$  is the pore velocity of gas phase. The above equations allow for the spatial and transient change of gas phase as well as the discrete differences among phase densities. As ice and hydrate phases are assumed incompressible and stationary, the internal energy is used for ice and hydrate phases. As gas phase flows through the

void space, enthalpy is used in equation (3) and volume expansion cooling (the second term on left hand side) has only the gas phase contribution. The inertia, advection of momentum and viscous terms are neglected in equation (2) since they are negligibly small compared to Darcy term.

The initial conditions are no flow and uniform pressure ( $P_i$ ) and temperature ( $T_i$ ) conditions. The boundary conditions for continuity and momentum equations are

$$v_G = 0 \quad \text{at } r = 0 \quad (4)$$

$$P = P_s \quad \text{at } r = r_o, \quad (5)$$

where  $P_s$  decreases linearly from  $P_i$  to  $P_f$  during interval  $t_{dep}$ . The thermal boundary conditions required for the energy equation are symmetry condition at the center and convection condition at outer surface:

$$\frac{\partial T}{\partial r} = 0 \quad \text{at } r = 0 \quad (6)$$

$$k_{eff} \frac{\partial T}{\partial r} = h_{eff} (T_s - T) \quad \text{at } r = r_o. \quad (7)$$

Equation (3) has the phase internal energy ( $u_k$ ), enthalpy ( $h_k$ ) and the temperature ( $T$ ) as dependent variables. As both the internal energy and enthalpy are thermodynamic properties, they are function of temperature, pressure and composition, and need to be eliminated for improved performance of numerical solution procedure. Temperature is preferred as a dependent variable because it is a measurable quantity, and the evaluation of the diffusive flux is not subject to the assumptions made on the specific heat and latent energy. Under the assumptions of the present study, the total enthalpy and internal energy are expressed as follows:

$$h_G = c_{p, gas CH_4} (T - T_{q1}) \quad (8)$$

$$u_I = c_{solid H_2O} (T - T_{q1}) \quad (9)$$

$$u_H = [c_{guest CH_4} (T - T_{q1}) + M] C_H + [c_{host H_2O} (T - T_{q1}) + N](1 - C_H). \quad (10)$$

The total enthalpy of methane gas and internal

energy of ice at  $T = T_{q1}$  are chosen to be zero as those two states represent the final condition of medium after full decomposition. The enthalpy difference between the pure substances is arbitrary, and the influence of pressure is. The total internal energy of hydrate phase is merely a mass averaged total internal energy of the partial specific total internal energy of constituents. The terms  $M$  and  $N$  are latent heat of methane and  $H_2O$  as guest and host molecules relative to the gas methane and ice at reference temperature, respectively. Both  $M$  and  $N$  are thermodynamic properties and generally vary with pressure and hydration number. But carefully calculated values based on experimental data showed that the heat of hydrate dissociation and hydration number are constant within experimental error over the entire (hydrate, liquid, vapor) coexistence region. [9] The mass concentration of methane in hydrate phase ( $C_H$ ) in equation (10) is related to the hydration number ( $n$ ) and molecular weight as follows:

$$C_H = \frac{\overline{M}(CH_4)}{n \cdot \overline{M}(H_2O) + \overline{M}(CH_4)}. \quad (11)$$

Equations (8) to (10) are now rewritten in terms of phase specific heat and latent energy:

$$h_G = c_{pG} (T - T_{q1}) \quad (12)$$

$$u_I = c_I (T - T_{q1}) \quad (13)$$

$$u_H = c_H (T - T_{q1}) - \Delta H_H \quad (14)$$

In the above equation,  $\Delta H_H$  is the heat of hydrate decomposition into ice and methane gas per unit mass of hydrate. Table 1 contains the values of physical properties employed in the present study.

	$\rho$ [kg/m <sup>3</sup> ]	$C_p$ [kJ/kg·K]	$k$ [W/mK]	$\Delta H$ [kJ]
G	-	2335	0.032	0
H	914	2530	2.35	-988
I	914	2085	0.5	0

Table 1. Thermophysical properties of each phase.

A few additional variables are defined below to put the transport equations in the simpler forms and for later use in the phase change model equations:

$$\rho = \sum_k \varepsilon_k \rho_k \quad (15)$$

$$h = \frac{1}{\rho} (\varepsilon_G \rho_G h_G + \varepsilon_I \rho_I u_I + \varepsilon_H \rho_H u_H) \quad (16)$$

$$c_p = \frac{1}{\rho} (\varepsilon_G \rho_G c_{pG} + \varepsilon_I \rho_I c_{pI} + \varepsilon_H \rho_H c_{pH}) \quad (17)$$

Finally, the macroscopic energy equation in terms of temperature is:

$$\begin{aligned} \frac{\partial}{\partial t} (\rho c_p T) + \frac{1}{r^2} \frac{\partial}{\partial r} (r^2 \varepsilon_G \rho_G v_G c_{pG} T) = \\ \frac{1}{r^2} \frac{\partial}{\partial r} (r^2 k_{eff} \frac{\partial T}{\partial r}) + \rho_H \Delta H_H \frac{\partial \varepsilon_H}{\partial t} + \frac{\partial}{\partial t} (\varepsilon_G P). \end{aligned} \quad (18)$$

### Thermal conductivity and permeability

The analytical determination of the effective thermal conductivity ( $k_{eff}$ ) and permeability (K) need the knowledge of detailed microscopic distribution of each phase and are very complicated even for the simple geometries. Due to the lack of the information regarding the morphology of the solid phases, the volume weighted conductivity model (or parallel resistance model) defined below is utilized,

$$k_{eff} = \sum_k \varepsilon_k k_k. \quad (19)$$

The permeability of hydrate pellet strongly depends on the fabrication method and parameters such as morphology of hydrate particles, porosity, compression pressure and temperature. The measured permeability of oil reservoir rocks ranges between  $10^{-11}$  and  $10^{-13}$  and that of fresh sandstone ranges between  $10^{-14}$  and  $10^{-15} m^2$ . [10] The measured porosity and permeability of R11 hydrate plugs artificially formed in glass pipe sections varied from 0.09 to 0.5 and from  $3.7 \times 10^{-11}$  to  $4.1 \times 10^{-15} m^2$ . [11] Therefore the influence of permeability on the predicted decomposition of hydrate pellet is estimated for the range between  $10^{-11}$  and  $10^{-15} m^2$  in the

present report.

### Phase Change Model

The macroscopic transport equations [equations (1), (2) and (18)] have three phase volume fractions as unknown variables in addition to the main dependent variable temperature. Additional relations are required to solve for the volume fractions of gas, ice and hydrate phases. One of the relations is that the sum of the phase volume fractions is unity and self-evident from the definition of the phase volume fraction:

$$\sum \varepsilon_k = 1. \quad (20)$$

Another relation is established on the assumptions of dry gas phase and stationary solid phases, which implies that mass of  $H_2O$  within a given local volume is conserved even though excessive evolved gas is discharged:

$$\rho_{H_2O} = \rho_I \varepsilon_I + \rho_H \varepsilon_H (1 - C_H) = const. \quad (21)$$

The other relation is obtained from the equilibrium phase diagram and the hydrate decomposition kinetics, and constitutes a phase change model.

If decomposition occurs at an extremely slow rate, the equilibrium phase relations in the below is valid.

Quadruple point:

$$P = P_{q1}, \quad T = T_{q1}. \quad (22)$$

Hydrate, ice and gas phase equilibrium line:

$$T = T_{eq}(P). \quad (23)$$

For  $H_2O - CH_4$  system, the equilibrium pressure and temperature along  $I - H - V$  lines are well documented. [2] In the present study the following relations are derived from a few experimental data and utilized:

$$P_{q1} = 2563 \text{ kPa}, \quad T_{q1} = 272.9 \text{ K} \quad (24)$$

$$T_{eq}(P) = \frac{2148}{15.72 - \ln P} [\text{K}].$$

If decomposition occurs at a considerable rate, the kinetic relation based on well known Kim-Bishnoi model [12] is valid:

$$\frac{d\bar{n}}{dt} = -k_0 \exp\left(-\frac{E}{RT}\right) A_s (f_{eq} - f) . \quad (25)$$

After employing expressions for hydrate mass and for surface area per unit volume from simple dimensional analysis;

$$m_H = \rho_H \varepsilon_H V = \bar{M}_H \bar{n} . \quad (26)$$

$$\frac{A_s}{V} = \frac{\varepsilon_H}{\sqrt{2K}} , \quad (27)$$

the final form of kinetic relation used in this work is as follows:

$$\frac{d\varepsilon_H}{dt} = k_T (T_{eq} - T) . \quad (28)$$

$$k_T = \frac{\bar{M}_H}{\rho_H} k_0 \exp\left(-\frac{E}{RT}\right) \frac{\varepsilon_H}{\sqrt{2K}} \left. \frac{\partial f}{\partial T} \right|_{eq} . \quad (29)$$

In the above equation the transient change in hydrate volume fraction is intentionally expressed in terms of the difference in equilibrium and local temperatures in order to be compatible with the numerical algorithm “enthalpy method”, which will be explained later. If the values of  $k_0 = 36 . kmol / (m^2 Pa \cdot s)$  and  $E=81kJ/mol$ , which were empirically determined by Clarke and Bishnoi [13] for the decomposition into liquid water and gas are used, the magnitude of  $k_T$  is about  $0.0085 s^{-1}K^{-1}$  for  $T = 263 .1K$  ,  $\varepsilon_{H=0.5}$  and  $K = 1. \times 10^{-12}$  . As the decomposition kinetic of hydrate into ice and gas phase is difficult to estimate exactly, the influence of intrinsic kinetics on the predicted decomposition of hydrate pellet is estimated for the  $k_T$  value range between 0.00085 and 0.0085 in the present work.

### Method of solution

The macroscopic energy equation (18) is a partial differential equation parabolic in time and elliptic in space coordinate. The marching type numerical procedure is utilized, in which successive update of various dependent variables are continued until the convergence criteria are satisfied at a given time step. Then the same iterative solution procedure is repeated for the new time step. The detailed procedure at a given time step is as follows.

1. To start the new time step, modify the time and surrounding pressure according to the depressurization schedule.
2. Determine phase volume fractions utilizing the algorithm “enthalpy method” satisfying equations (20), (21) and (28).
3. Update gas density and other properties.
4. Solve continuity and momentum equations for pressure and velocity field utilizing the algorithm based on SIMPLE method. [14]
5. Solve energy equation for temperature.
6. Check convergence. Go to *step 2* if not converged.
7. Move to next time step.

The predictor-corrector type algorithm “enthalpy method” which was suggested by Voller [15] to take into account the couplings among temperature, enthalpy and phase volume fractions is extended and employed in *step 2*. The phase volume fractions are updated in such a way that the nodal value of  $\rho h$  and  $\rho_{H_2O}$  remain unchanged under the constraint of kinetic relation [equation (28)]. The diagram shown in Figure 2 depicts how hydrate volume fraction is determined from current values of  $\varepsilon_H^*$  ,  $T^*$  in extended enthalpy method. Despite  $\rho h$  is the combination of internal energy and enthalpy of different phases, the algorithm is conveniently called enthalpy method considering the possible extension to the moving solid phase circumstances.

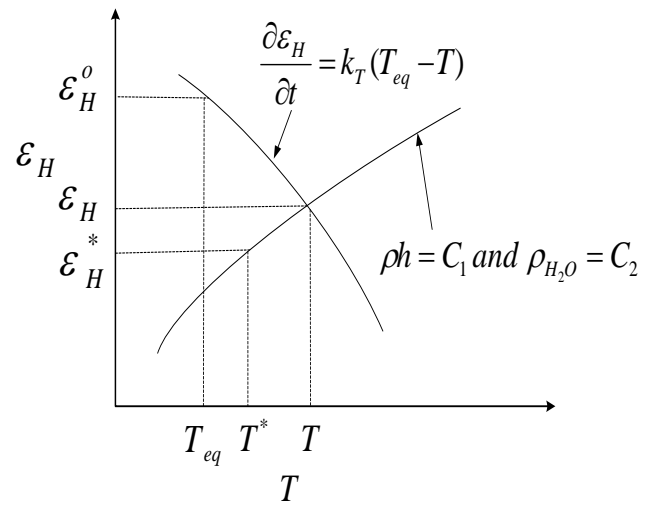


Figure 2 The diagram of enthalpy method extended for non-equilibrium decomposition.

In *step 6*, the convergence criterion requires that the changes in the average total enthalpy of the system ( $\overline{\rho h}$ ) relative to the previous iteration normalized with the present iteration value is smaller than  $1. \times 10^{-12}$ , which is defined as

$$\overline{\rho h} = [\sum \rho h \Delta V] / \sum \Delta V . \quad (30)$$

For the predicted results discussed in this paper, the number of calculation grid is 202. The time step is about 1 s initially and is gradually increased using the relation

$$\Delta t = 0.0589 (t + 288)^{0.5} . \quad (31)$$

## RESULTS AND DISCUSSION

### System parameters

The parameters which affect the decomposition of hydrate are pellet radius, porosity, permeability, initial temperature, depressurization schedule ( $P_i$ ,  $P_f$ ,  $t_{dep}$ ), intrinsic kinetic coefficient, convective heat coefficient and temperature of surrounding medium. Numerical implementations were conducted for different combinations of pellet radius ( $R$ ), permeability ( $K$ ), convective heat transfer coefficient ( $h_{eff}$ ) and kinetic coefficient ( $k_T$ ). Table 2 summarizes the system parameters of cases discussed in the present paper. For all cases, the initial and surrounding medium temperature is fixed at 263.1 K. Also the initial pressure, final pressure and time to achieve the final pressure does not change;  $P_i = 5000 \text{ kPa}$ ,  $P_f = 1000 \text{ kPa}$  and  $T_{dep} = 1000 \text{ s}$ .

### Transient change in temperature and flow field

Transient changes in radial distribution of temperature for Case 2 is shown in Figure 3. The cooling effect due to gas phase expansion is not noticeable for the tested conditions. When the surrounding pressure drops below the equilibrium pressure corresponding to the initial temperature the hydrate temperature starts to decrease along the three phase equilibrium curve of P-T diagram. During the depressurization period medium temperature has almost uniform distribution. As the complete decomposition of hydrate occurs earlier in the outer portion compared to the region near the center, the medium temperature starts to

Series	R [m]	K [m <sup>2</sup> ]	$h_{eff}$ [W/m <sup>2</sup> K]	$k_T$ [1/sK]
1	0.01 0.02 0.03 0.04 0.05	$1.0 \times 10^{-13}$	100.0	0.0085
2	0.02	$1.0 \times 10^{-13}$ $1.0 \times 10^{-14}$ $1.0 \times 10^{-15}$	100.0	0.0085
3	0.02	$1.0 \times 10^{-13}$	100.0	0.00027 0.00085 0.0085
4	0.02	$1.0 \times 10^{-13}$	10.0~ 200.0	0.0085

Table 2. Summary of predicted conditions.

increase towards the surrounding temperature due to convective heating. When the decomposition of all hydrate is complete the temperature of ice phase within pellet increases in radial direction. Radial distribution of mass flow rate shown in Figure 4 clearly indicates that decomposition of hydrate and liberation of gas phase is volumetric phenomena. Decomposition occurs for the entire volume of the pellet while the surrounding pressure is decreasing. And mass flow rate of evolved gas phase monotonically increases in radial direction. After the surrounding pressure reaches the final pressure the decomposition of hydrate takes place within the spherical shell region surrounded by already decomposed region. The decomposition of core region is suspended until the heat flux supplied by the surrounding medium reaches this region via heat conduction.

### Influence of pellet size and permeability

Figure 5 represents the influence of pellet radius on dissociation completion time for Cases 1 through 5. The time required for the completion of decomposition (decomposition time) is roughly proportional to pellet radius. When pellet radius varies from 10 mm to 50 mm the decomposition time increases roughly five times.

Figure 6 shows the influence of permeability on accumulated gas production. When permeability is larger than  $1. \times 10^{-14}$  decomposition of hydrate pellet is insensitive to the changes in permeability.

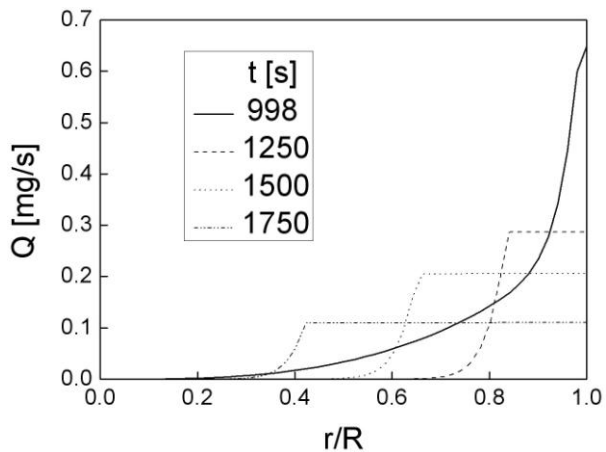


Figure 4 Radial distribution of mass flow rate at some time instances during series 1 and  $R=0.02$

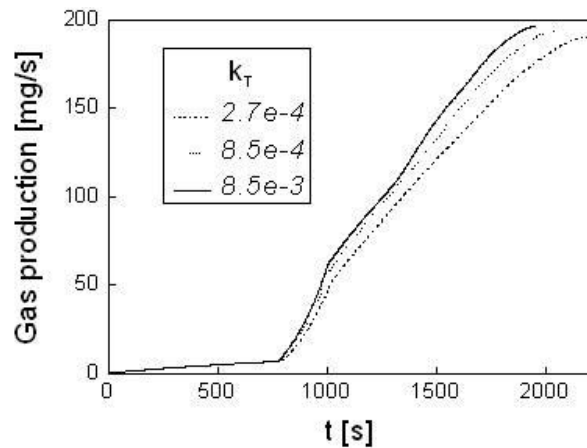


Figure 7 Influence of intrinsic kinetic rate on accumulated gas production

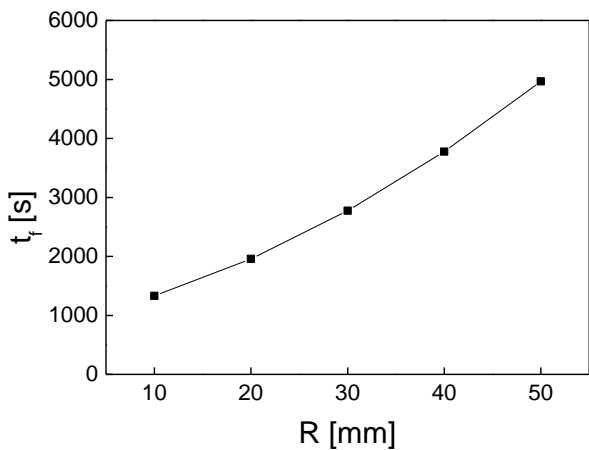


Figure 5 Influence of pellet radius on dissociation completion time for series 1

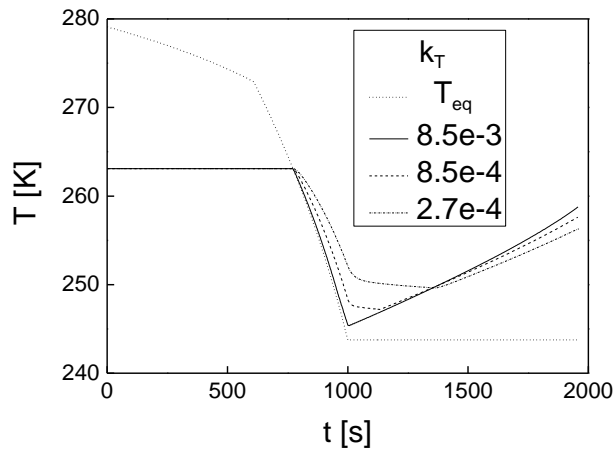


Figure 8 Influence of intrinsic kinetic rate on pellet surface temperature

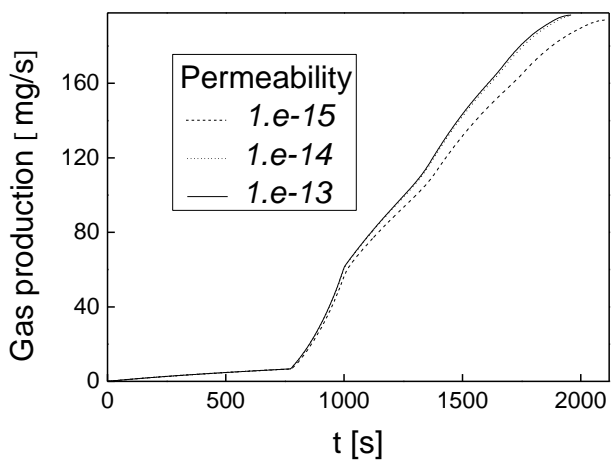


Figure 6 Influence of permeability on accumulated gas production

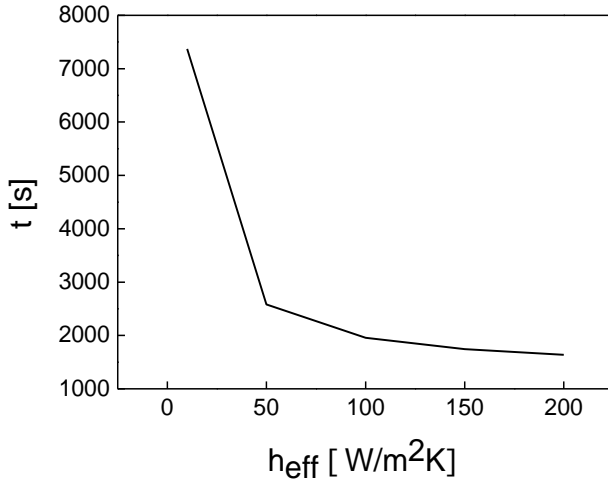


Figure 9 Effect of convection coefficient on decomposition time.

Permeability smaller than this value delays the decomposition. The change in permeability from  $1. \times 10^{-14}$  to  $1. \times 10^{-15}$  caused the decomposition time change from 1973 s to 2107 s.

### Influence of kinetic coefficient

As kinetic rate decreases the decomposition time increases (Figure 7). Since one order of magnitude increase in kinetic coefficient is equivalent to two orders of magnitude decrease in permeability according to equation (29), the tested range of kinetic constant in Figure 7 is equivalent to three orders of magnitude change in permeability. Therefore, the influence of kinetic rate must not be determined independent with the influence of permeability. The predicted results shown in Figures 7 and 8 is valid only under the condition of sufficiently large permeability. If the kinetic rate coefficient is as small as  $2.7 \times 10^{-4}$ , the medium temperature can be several degrees larger than equilibrium temperature during hydrate decomposition (Figure 8).

### Effects of convective heating

Decomposition time decreases almost exponentially as the effective heat transfer coefficient at the bounding surface increases (Figure 9). In other words the effect is more drastic for relatively small  $h_{eff}$ . The decomposition time decreases from 7370 s to 2581 s when  $h_{eff}$  changed from 10 to 50 W/mK.

### CONCLUSIONS

Mathematical model based on the conservation principles, the phase equilibrium relation, equation of gas state and phase change kinetics and its numerical implementation employing single-domain approach, volume average formulation and extended enthalpy algorithm has revealed essential features of hydrate pellet decomposition. Finally system parameters affect the heat and mass transfer occurring during non-equilibrium decomposition of hydrate pellet in the following ways for the tested ranges of parameters:

1. The cooling effect due to gas phase expansion is not noticeable.
2. Decomposition of hydrate and liberation of gas phase is volumetric phenomena.

3. The time required for the completion of decomposition (decomposition time) is roughly proportional to pellet radius.
4. The influence of permeability larger than  $1. \times 10^{-14}$  on decomposition of hydrate pellet is negligible. As permeability decreases smaller than this value, the time for complete decomposition increases.
5. Even though, the changes in intrinsic kinetic and permeability are dependent to each other through microscopic surface area per unit volume, it is valid that the slower kinetic rate increases the time for complete decomposition under the condition of sufficiently large permeability.
6. Decomposition time decreases almost exponentially as the effective heat transfer coefficient at the bounding surface increases.

### ACKNOWLEDGEMENT

The authors are grateful for financial support to Korean Ministry of Knowledge Economy. They also like to thank the following companies: Daewoo E&C, Hyundai Eng. Co., SK E&C, Samsung Heavy Industry co. and Sung Il co.

### REFERENCES

- [1] Iwasaki T., Ketoh Y., Nagamori S., Takahashi S. and Oya N. *Continuous natural gas hydrate pellet production (NGHP) by process development unit (PDU)*. In: *Proceedings of the Fifth International Conference on Gas Hydrates, Trondheim, 2005*.
- [2] Sloan ED. and Koh CA. *Clathrate hydrates of natural gases 3<sup>rd</sup> ed.* Boca Raton: CRC Press, 2007.
- [3] Kelkar SK., Selim MS. and Sloan ED. *Hydrate dissociation rates in pipelines*. Fluid Phase Equilibria 1998;150-151:371-382.
- [4] Peters D., Metha A. and Walsh J. The physics of hydrate plug dissociation: a comprehensive model based upon facts, conjecture and field experience. In: *Proceedings of the Fourth International Conference on Gas Hydrates, Yokohama, 2002*.
- [5] Dicharry C., Gayet P., Marion G., Graciaa A. and Nesterov AN. *Modeling heating curve for gas hydrate dissociation in porous media*. J. Phys. Chem. B 2005;109:17205-17211.
- [6] Sun X. and Mohanty KK. *Kinetic simulation of methane hydrate formation and dissociation in*

*porous media*. Chemical Engineering Science 2006;61:3476-3495.

[7] Gerami S. and Pooladi-Darvish M. *Predicting gas generation by depressurization of gas hydrates where the sharp-interface assumption is not valid*. J. Petroleum Sci. and Eng. 2007;56:146-164.

[8] Drew DA. *Mathematical modeling of two-phase flow*. Ann. Rev. Fluid Mechanics 1983;15:261-291.

[9] Anderson GK. *Enthalpy of dissociation and hydration number of methane hydrate from the Clapeyron equation*. J. Chem. Thermodynamics 2004;36:1119-1127.

[10] Bear J. *Dynamics of fluids in porous media*. New York: American Elsevier Publishing co., 1972.

[11] Berge LI., Gjertsen LH. and Lynse D. *Measured permeability and porosity of R11 hydrate plugs*. Chemical Engineering Science 1998;53(9):1631-1638.

[12] Kim HC., Bishnoi PR., Heideman RA. and Rizvi SSH. *Kinetics of methane hydrate decomposition*. Chemical Engineering Science 1987;42:1645-1653.

[13] Clarke M. and Bishnoi PR., *Determination of the activation energy and intrinsic rate constant of methane gas hydrate decomposition*. Canadian J. Chem. Eng. 2001;79:143-147.

[14] Panankar S. *Numerical Heat transfer and fluid flow*. New York: Hemisphere Publishing co., 1980.

[15] Voller VR., Cross M. and Markaios NC. *An enthalpy method for convection/diffusion phase change*. Int. J. Num. Math. Eng. 1987;24:2